High-Resolution AFM of Membrane Proteins Directly Incorporated at High Density in Planar Lipid Bilayer

Pierre-Emmanuel Milhiet,* Francesca Gubellini,† Alexandre Berquand,† Patrice Dosset,* Jean-Louis Rigaud,† Christian Le Grimellec,* and Daniel Lévy†

*Centre de Biochimie Structurale, Groupe Nanostructures et Complexes Membranaires, UMR 554 INSERM, UMR 5048 CNRS, Montpellier, France; and †Institut Curie, UMR-CNRS 168 and LRC-CEA 34V, 75248 Paris Cedex 05, France

ABSTRACT The heterologous expression and purification of membrane proteins represent major limitations for their functional and structural analysis. Here we describe a new method of incorporation of transmembrane proteins in planar lipid bilayer starting from 1 pmol of solubilized proteins. The principle relies on the direct incorporation of solubilized proteins into a preformed planar lipid bilayer destabilized by dodecyl-β-maltoside or dodecyl-β-thiomaltoside, two detergents widely used in membrane biochemistry. Successful incorporations are reported at 20°C and at 4°C with three bacterial photosynthetic multisubunit membrane proteins. Height measurements by atomic force microscopy (AFM) of the extramembraneous domains protruding from the bilayer demonstrate that proteins are unidirectionally incorporated within the lipid bilayer through their more hydrophobic domains. Proteins are incorporated at high density into the bilayer and on incubation diffuse and segregate into protein close-packing areas. The high protein density allows high-resolution AFM topographs to be recorded and protein subunits organization delineated. This approach provides an alternative experimental platform to the classical methods of two-dimensional crystallization of membrane proteins for the structural analysis by AFM. Furthermore, the versatility and simplicity of the method are important intrinsic properties for the conception of biosensors and nanobiomaterials involving membrane proteins.

INTRODUCTION

Membrane proteins have a pivotal role in such cellular processes as energy transfer, cell homeostasis, signal transduction, and cell communication and are highly relevant to human physiology and disease (e.g., depression, stroke, diabetes, multi-drug resistance). Although the magic number of 100 atomic structures solved has recently been reached (http://blanco.biomol.uci.edu/Membrane_Proteins_xtal.html), compared to several thousands for cytoplasmic ones, a major challenge remains in the difficulties of heterologous overexpression of membrane proteins, especially from eukaryotic organisms, in large amount for structural analysis (1). To bypass this limitation, technical improvements in miniaturization and robotization for three-dimensional (3D) crystallization allowed decreasing the amount of protein to tens of nanograms per trial. In 2D crystallization, strategies have been developed to concentrate proteins present in bulk at the air/water interface, thereby decreasing the amount of protein to 1 μg per trial (2,3). However, because crystallization requires a large number of trials, milligrams of purified proteins are usually required.

In this context, atomic force microscopy (AFM) represents a technique complementary to x-ray crystallography and electron microscopy in membrane protein research (4,5). With AFM, topographies of membrane proteins can be acquired at subnanometer lateral and $\sim$1 Å vertical resolutions in near physiological conditions. Furthermore, AFM allows analysis of the flexibility and the conformational changes of extrinsic domains. By applying loading forces to the AFM tip, biological samples can be nanodissected to provide insights into protein assembly (6,7). Finally, force spectroscopy measurements allow delineating the intramolecular interactions that stabilize the proteins into lipid bilayers (8,9).

So far, AFM studies have been performed with purified membrane proteins reconstituted into lipid bilayers as 2D crystals and, in a few cases, with densely packed proteins in native specialized membranes (6,10,11). From these studies, it can be stressed that the high density of incorporated proteins and the flatness and the large size of membranes $>$200 nm are prerequisites for subnanometer-resolution AFM. Experimentally, 2D crystals are formed by reconstitution of protein in a lipid bilayer at high protein/lipid ratio on detergent removal from a fully solubilized lipid/ protein/ detergent mixture. Although reconstitution of proteins into liposomes at low protein/lipid ratio for functional studies is well established (for a recent review see Rigaud and Levy (12)), reconstitution at high protein density remains empirical and often leads to protein aggregations or to vesicles too small for AFM analysis. Other approaches have produced protein-containing planar lipid bilayers on solid surfaces for functional analysis or for nanobiotechnology applications (13,14). However, as analyzed by single-molecule

Submitted May 9, 2006, and accepted for publication July 11, 2006.

Address reprint requests to Dr. Daniel Lévy, Laboratoire Physico-Chimie, UMR168 CNRS/Institut Curie, 75231 Paris Cedex 05, France. Tel.: 33-142-34-67-82; Fax: 33-140-51-06-36. E-mail: daniel.levy@curie.fr, or to Dr. Pierre-Emmanuel Milhiet, Centre de Biochimie Structurale, UMR554 INSERM, UMR5048 CNRS, 34090, Montpellier, France. Tel.: 33-467-41-79-17; Fax: 33-467-41-79-13; E-mail: pem@cbs.cnrs.fr.

0006-3495/06/11/3268/08 $2.00

doi: 10.1529/biophysj.106.087791

fluorescence, protein density is usually too low for high-resolution AFM (15).

Here, we report a new method of incorporation of membrane proteins into a planar lipid bilayer allowing AFM analysis at high resolution. The principle, derived from our studies of direct incorporation into liposomes (12,16), is based on insertion of proteins into a planar lipid bilayer after destabilization by sugar-based detergents. The method is illustrated with the successful reconstitution of three membrane proteins from the bacterial photosynthetic apparatus, a light-harvesting complex 2 (LH2) and two light-harvesting complex 1 (LH1) reaction center (RC), also named core complexes. Height measurement by AFM of extramembranous domains pointing out the lipid bilayer reveals that all proteins are unidirectionally incorporated in the lipid bilayer. Compared to previous work on reconstitution on solid supports, including tethered lipid bilayers (13,14), proteins are incorporated at high density, allowing high-resolution AFM topographs to be acquired. As a major result, the amount of protein per incorporation trial is extremely low, $\sim 10^{-12}$ mole of protein. Thus, this strategy appears very powerful for the structural analysis by AFM of membrane proteins expressed in low amount and for the conception of biomaterial involving membrane proteins.

MATERIALS AND METHODS

Dioleoyl-phosphatidylcholine (DOPC) and dipalmitoyl-phosphatidylcholine (DPPC) were of the highest purity and purchased from Avanti Polar Lipids (Alabaster, AL). *N*-octyl-β-D-glucoside (OG), dodecyl-β-D-maltoside (DDM), and dodecyl-β-D-thiomaltoside (DOTM) were purchased from Anatrace (Maumee, OH), and mica from Goodfellow (Lille, France).

Protein purification

LH2 and LH1-RC core complexes were purified from photosynthetically grown *Rhodobacter sphaeroides* (*Rb. sph.*) *pufX*-deleted strain and from *Rhodobacter veldkampii* (*Rb. veld.*), as previously described (17). Briefly, chromatophores were solubilized in 3% DDM or DOTM, and LH2 and LH1-RC photosynthetic complexes were separated according to their density by sedimentation in a sucrose gradient (10–35%) in 0.1% DOTM or in 0.1% DDM, 50 mM glycine-glycine, pH 7.8. The two bands corresponding to solubilized LH2 and LH1-RC were extracted from the sucrose gradient and kept frozen at −80°C. Solubilized complexes show typical near-infrared peaks for LH2 at 804 nm and 854 nm (LH2) and for LH1 (Qy at 884 nm and Qx at 592 nm) and for RC (bacteriochlorophyl at 804 nm and bacteriopheophytin at 760 nm). The solubilized complexes were stable several days at 4°C as revealed by the unmodified spectra of LH2 and of LH1-RC without appearance of a peak at 820 nm typical of dissociated LH subunits (17).

LH2 and LH1-RC concentrations were determined by spectroscopy from the absorption peaks at 850 nm ($\varepsilon = 382\ \mathrm{mM^{-1}cm^{-1}}$) and at 878 nm ($\varepsilon = 4.8\ \mathrm{mM^{-1}cm^{-1}}$), respectively.

SLBs preparation

Supported lipid bilayers (SLB) were prepared as reported previously (18). DOPC/DPPC (1:1 mol/mol) liposomes prepared by extrusion at 70°C of multi-lamellar vesicles at 0.125 mM in phosphate buffer, pH 7.4, were deposited onto freshly cleaved mica and allowed to adsorb and fuse during 2 h of incubation at 70°C. Before AFM experiments, the 10-mm diameter mica sheet was glued onto a 15-mm diameter wafer.

Direct incorporation of proteins

The stability of SLB in the presence of detergent was analyzed after incubation with a 50-μl drop of buffer, 10 mM Tris, 150 mM KCl, pH 7.4, and OG, DDM, and DOTM at different concentrations. After 15 min of incubation at room temperature that allowed the equilibration of the detergent between the volume and the lipid bilayer, the detergent was removed by extensive rinsing with a detergent-free buffer (30 drops of 50 μl).

For direct incorporation of proteins at room temperature, SLB were first rinsed by a 50-μl drop of buffer containing detergent above the critical micelle concentration (cmc) and 0.075 mM DOTM or 0.3 mM DDM for incorporations mediated by DOTM or DDM, respectively. Then SLB was incubated with a 50-μl drop of buffer, 10 mM Tris, pH 7.4, 150 mM KCl, containing solubilized proteins at 2–10 μg/ml (0.9 to 1.5 pmol) and 0.075 mM DOTM or 0.3 mM DDM. After 15 min of incubation allowing protein incorporation into the SLB, detergent was removed from the buffer and the SLB by extensive rinsing with a detergent-free buffer. The full reconstitution process including the previous rinsing step with detergent, incubation in the presence of solubilized proteins, and detergent removal takes 30 min.

For direct incorporation at 4°C, SLB was first preincubated 30 min with detergent below the cmc, 0.025 mM DOTM or 0.1 mM DDM to ensure a complete equilibration of the detergent within the SLB. Then, SLB was incubated 15 min with a 50-μl drop of buffer, 10 mM Tris, pH 7.4, 150 mM KCl, containing solubilized proteins at 2–10 μg/ml (0.9 to 1.5 pmol) and 0.075 mM DOTM or 0.3 mM DDM, followed by a detergent removal step by buffer rinsing.

Instabilities in the AFM signal when detergents were still present in SLB and in the buffer have prevented the analysis of the morphology of the SLB destabilized by detergents and the direct observation of the protein incorporation. Thus, all AFM topographs of the reconstituted samples were recorded after detergent removal.

The SLB-containing proteins were analyzed just after and up to 1–10 days after the detergent removal. The samples covered with a drop of buffer were kept at 4°C in a humid Petri dish between experiments to avoid evaporation of the buffer.

Atomic force microscopy imaging

Imaging was performed in the reconstitution buffer with commercial Nanoscope E or IIIa AFMs (Veeco, Santa Barbara, CA) equipped with a J scanner and oxide-sharpened Si_3N_4 sharp cantilevers ($k = 0.09$ N/m, Olympus, Japan; or $k = 0.1$ N/m, Veeco). The AFM was operated in contact mode, applying forces below 100 pN at a scan frequency of 4–6 Hz or in tapping mode at a scan frequency of 1 Hz. An average of LH1-RC reported in Fig. 3 *c* was calculated from the trace and retrace topographs using the Xmipp single-particle analysis program package (19).

RESULTS

We have previously analyzed in detail the mechanism of direct incorporation in bulk of different types of solubilized membrane proteins into detergent-destabilized liposomes (12,16). Direct incorporation was specifically triggered by sugar-based detergents, OG or DDM, added to the liposomes at a saturation concentration, i.e., before the onset of solubilization. We now extend this concept to the direct incorporation of membrane proteins into a planar lipid bilayer.

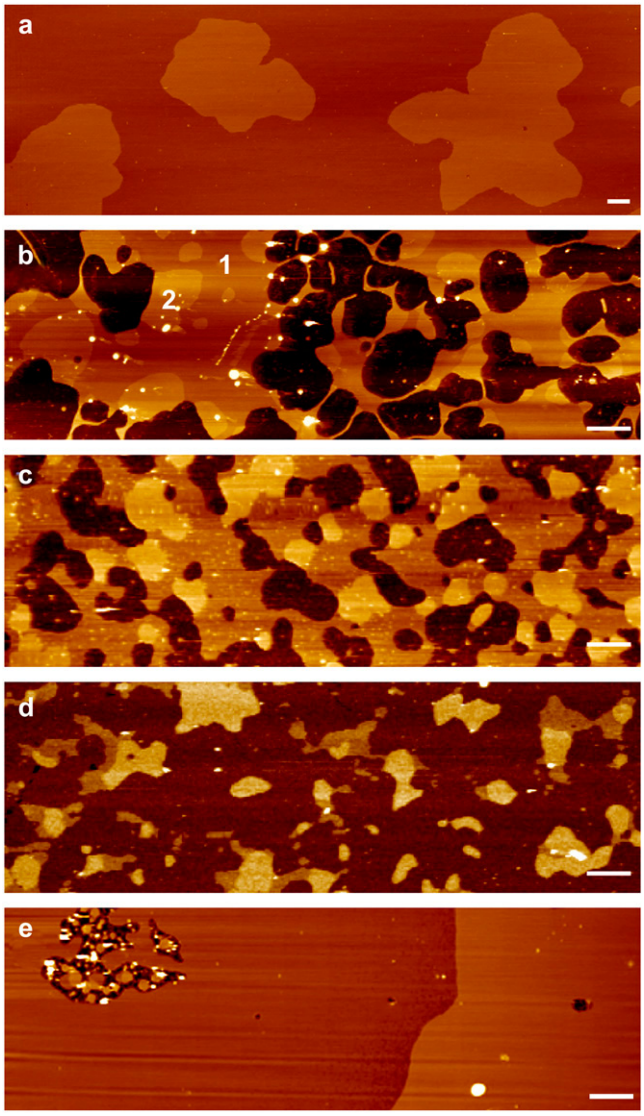

FIGURE 1 Interactions of SLB with sugar-based detergents at concentrations above the cmc. (*a*) Contact-mode imaging of DOPC/DPPC SLB. Lipid phase separation was observed between the darker DOPC fluid phase and the DPPC gel phase. (*b*) SLB after incubation at room temperature with 0.075 mM (1.5 × cmc) DOTM. Both fluid (*1*) and gel (*2*) phases were conserved; the darker areas were the mica, and the white dots nonfused vesicles. (*c* and *d*) SLB after incubation at room temperature (*c*) with 0.3 mM (1.7 × cmc) DDM and (*d*) with 17 mM (1 × cmc) OG. (*e*) SLB after incubation at 4°C with 0.075 mM DOTM. Detergents were removed by extensive rinsing before AFM imaging. *a*, *b*, and *e* were obtained in contact mode; *c* and *d* in tapping mode. The *z* color scale is 15 nm, and scale bars are 1 μm.

The experimental protocol involves three steps. First, a continuous and flat SLB is formed by fusion of vesicles onto mica. Then, the SLB is incubated with solubilized proteins and detergent at a concentration allowing the saturation of SLB. Proteins are incorporated at this step in the detergent-destabilized SLB. In the case of very low concentration of lipid as in the case of SLB, the concentration of detergent needed to saturate a lipid bilayer can be estimated slightly above the cmc (16). Finally, the detergent present in the bulk and in the SLB is removed by extensive rinsing by buffer exchange, and the sample is imaged by AFM. We thus first analyzed the interactions of SLB with OG, DDM, and DOTM, three detergents widely used in membrane biochemistry and crystallization, at concentrations close to the cmc.

SLB-detergent interaction

SLBs were formed by fusion in solution of vesicles composed of a binary mixture of DOPC and DPPC (1:1 mol/mol). The flat and continuous SLB with recognizable lipid phase separation at room temperature is depicted in Fig. 1. Micrometer DPPC gel-phase domains of irregular shapes protruded from the fluid DOPC matrix by 0.96 ± 0.16 nm ($n = 39$). This value is consistent with those reported from AFM (20) or from neutron diffraction (21) experiments.

SLBs were incubated with detergent 15 min at room temperature, allowing equilibration of detergents between the SLB and the buffer; then the detergent was removed by rinsing with a detergent-free buffer, and the lipid bilayer was analyzed by AFM. Results showed that, as pure lipid liposomes, SLBs were destabilized up to complete solubilization with increasing concentration of detergent. However, important differences in the solubilization process were found between the high-cmc detergent OG, cmc 17 mM, and the low-cmc detergents DDM and DOTM, cmc 0.17 mM and 0.05 mM, respectively.

Upon incubation with DDM or DOTM at a concentration above the cmc, 0.3 mM (1.7 × cmc) or 0.075 mM (1.5 × cmc), respectively, large interconnected bilayer areas several micrometers in size, corresponding to ~50% of the initial SLB, remained adsorbed onto the mica (Fig. 1, *b* and *c*). Gel- and fluid-phase domains were still present as judged by ~1 nm height difference between microdomains. However, large morphological changes of the membrane occurred; e.g., DPPC domains were of smaller size but in larger proportion than in the control SLB (50% vs. 30% in nontreated SLBs), likely because of the low accessibility of detergent in the tightly packed lipid phase. Cross-section analysis revealed 6.15 ± 0.93 nm ($n = 29$) height differences between DPPC domains and mica. According to the DPPC bilayer thickness of 4.42 nm measured by x-ray diffraction (22), SLB were supported by a water layer of at least 1.7 nm. Increasing concentrations of DDM or DOTM increased the amount solubilized up to the full solubilization at detergent concentrations well above the cmc (10 × cmc).

In the case of OG, only 10–15% of its surface was preserved (Fig. 1 *d*) after incubation with 17 mM OG (1 × cmc), whereas with 20 mM OG (1.15 × cmc), full solubilization of the SLB occurred. Finally, SLB was much more resistant at 4°C, where only small areas in the SLB were solubilized after incubation with 0.075 mM DOTM (Fig. 1 *e*).

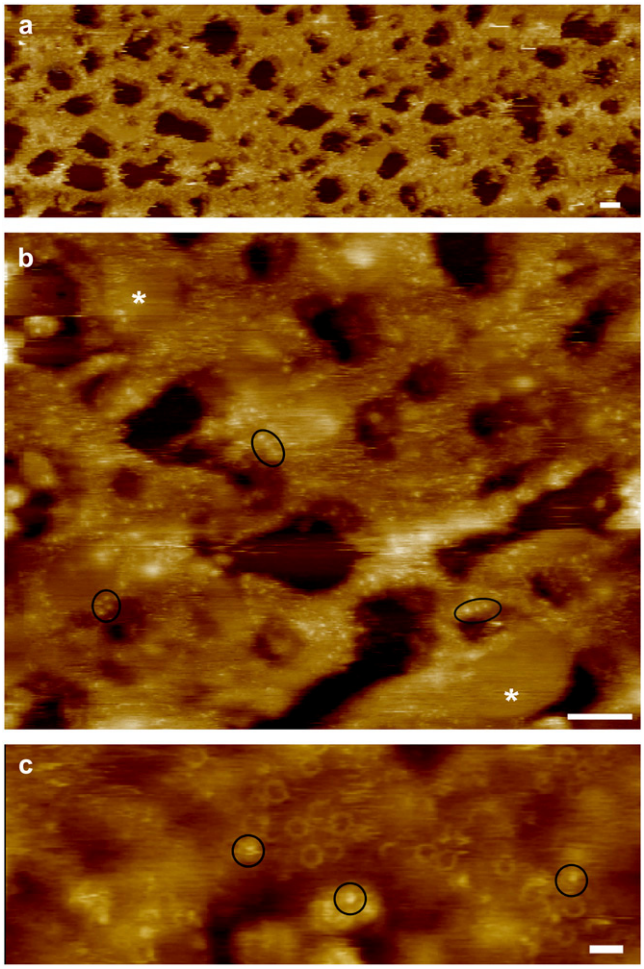

FIGURE 2 Direct incorporation of LH1-RC from *Rb. veld.* into SLB at room temperature. DOPC/DPPC SLB was incubated with 0.075 mM DOTM and 1.5 pmol of solubilized LH1-RC before detergent removal. (*a*) Low-magnification AFM contact-mode topograph reconstituted SLB consisted of interconnected lipidic domains without bound vesicles or protein aggregates. (*b*) Higher magnification revealed DPPC domains (*asterisks*) and corrugated domains containing LH1-RC complexes (*bright yellow dots*). Protein density was variable, and several proteins were in close contact (*black ellipses*). (*c*) High-resolution AFM topographs of empty LH1 rings and LH1-RC complexes (*dark circles*). The *z* color scale is 15 nm (*a* and *b*) or 10 nm (*c*); the darker areas correspond to the mica. Scale bars are 100 nm in *a* and *b* and 20 nm in *c*.

Because SLB were more resistant to DDM and DOTM at concentrations above the cmc, we evaluated the incorporation of proteins after destabilization of SLB with those detergents.

Direct incorporation of membrane proteins at room temperature

Three membrane proteins from the bacterial photosynthetic apparatus were tested, namely LH2 (MW ~110 kDa) from *pufX*-deleted *Rhodobacter sphaeroides* (*puf*X$^-$-*Rb. sph.*) and LH1-RC core complexes (MW ~300 kDa) from *puf*X$^-$-*Rb. sph.* and from *Rb. veld.* These membrane proteins are structurally known from x-ray, electron crystallograpy, and/or AFM experiments, and their particular shapes are recognizable in AFM topographs (11,23). LH2 forms a transmembrane ring 6 nm in diameter constituted of nine heterodimers of the single membrane-spanning α-and β-subunits (24). LH1-RC from *puf*X$^-$-*Rb. sph.* is a monomeric complex constituted by a LH1 ring of ~10 nm of 16 α- and β-heterodimers and surrounding the RC (23). LH1-RC from *Rb. veld.* has recently been purified, but the oligomeric state is not yet characterized.

We first tried incorporations of solubilized LH1-RC (1–5 pmol) after destabilization of SLB with DOTM below the cmc, 0.02–0.01 mM at room temperature. After detergent removal, SLB showed minor modifications compared to untreated SLB with too few protrusions to allow an unambiguous assignment of incorporated proteins (data not shown).

Then, we performed incorporation trials of solubilized LH1-RC from *Rb. veld.* (1.5 pmol) into SLB destabilized with DOTM above the cmc (0.075 mM). Instabilities in AFM analysis when detergent was still present in the lipid bilayer have prevented direct observation of the incorporation process. After detergent removal, low-magnification topographs revealed that the protein-incubated SLB had been only partly solubilized, as observed after incubation with detergent alone (Fig. 2 *a*). The remaining lipid bilayer was flat and constituted of 200 nm $\times$ 200 nm areas interconnected along several micrometers without any protein aggregates or bound vesicles. In a control experiment, a mixture of fully solubilized lipid and protein in 0.075 mM DOTM and at medium lipid/protein ratio, i.e., 2 w/w, was added in solution onto freshly cleaved mica, followed by a rinsing step, led to a clean surface. This confirmed that the interconnected bilayers resulted from the initial planar lipid membrane and not from proteoliposomes reconstituted in bulk and further fused onto the mica.

At medium magnification, smooth areas (*asterisks* in Fig. 2 *b*) alternated with highly corrugated domains. The former, with a 6.9-nm height from the mica, were assigned to pure DPPC. The latter were constituted of lipid areas in which a high amount of LH1-RC, as seen as bright dots pointing out of the membrane, has been incorporated. LH1-RC protruded 3.0 $\pm$ 0.5 nm (n = 23) above the lipid bilayer, a value consistent with those reported for the cytoplasmic side of the H subunit of the RC (11,25) (see also Fig. 1 *b*). Proteins were never found in DPPC domains and were present along the full bilayer, i.e., along tens of micrometers. The protein-protein distances were variable, indicating a heterogeneous protein distribution within the bilayer, and several proteins were in close contact with a protein-protein distance below 14 nm (*black ellipses* in Fig. 2 *b*).

Higher-magnification topographs showed LH1-RC constituted of monomeric empty LH1 rings of 9.9 $\pm$ 1.2 nm (n = 30) top-ring diameter, a size similar to several bacterial core complexes (11). As already observed (11,25), the H subunit

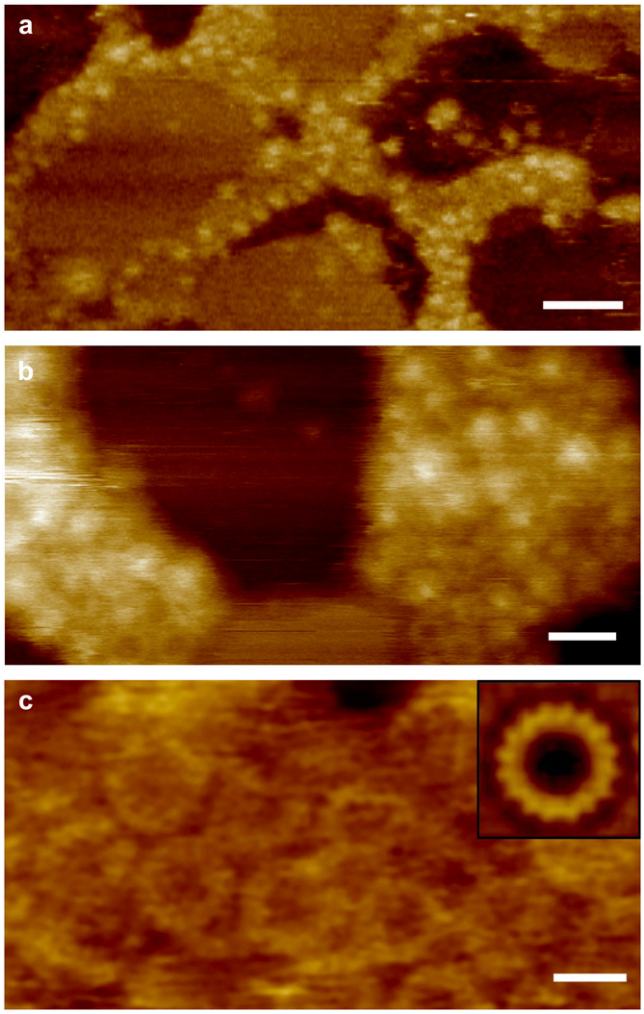

FIGURE 3 Membrane remodeling and high-resolution AFM imaging of core complexes. (*a*) Tapping mode of the same membrane as in Fig. 2 after 24 h of incubation at 4°C, revealing that proteins have been segregated into close-packing areas. (*b*) Higher-magnification AFM topograph where most of the core complexes contained the H subunit topping the RC underlining a preferential orientation of protein insertion. (*c*) High-resolution AFM analysis of LH1-RC from *pufX*$^{-}$-*Rb. sph.* after direct incorporation into SLB. The H subunit of RC was removed by the AFM tip in contact mode, revealing the 16 α/β-heterodimers of LH1 in the average image (*inset*). The *z* color scale corresponds to 20 nm, and the scale bars in *a*, *b*, and *c* are 50 nm, 20 nm, and 10 nm, respectively.

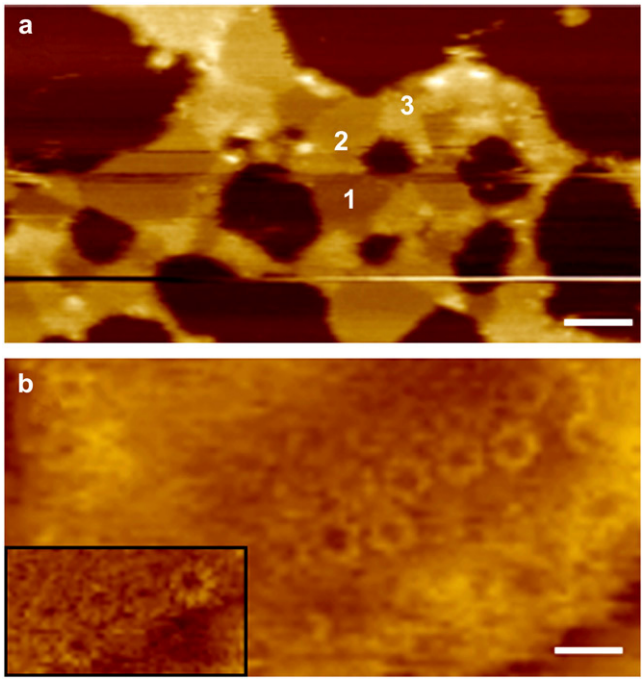

FIGURE 4 High-resolution AFM imaging of LH2 after direct incorporation into SLB. SLB was incubated at room temperature with 0.075 mM DOTM and 0.9 pmol of solubilized LH2 before detergent removal. (*a*) Low-magnification AFM contact-mode image of SLB shows DOPC domains (*1*), DPPC domains (*2*), and more corrugated domains (*3*) containing LH2 at high density. (*b*) High-resolution topographs of packed LH2 where the nine α/β-pairs of LH2 were resolved in raw data (*inset*). The vertical color scales correspond to 20 nm (*a*) or 7 nm (*b*). The scale bars represent 100 nm (*a*) or 10 nm (*b*).

topping the central RC that was present in the low-resolution topographs has likely been removed by the AFM tip during the scanning at too large loading forces. This was confirmed by the presence of few full core complexes with a central RC surrounding a less resolved LH1 ring (Fig. 2 *c*, *dark circle*) and in topographs acquired in oscillating mode (Fig. 3 *b*) or in contact mode at lower loading forces (Fig. 5 *b*).

Similar reconstitutions were also performed with LH1-RC or with LH2 from *pufX*$^{-}$-*Rb. sph.* after destabilization of SLB with DOTM above the cmc, leading to large interconnected membranes containing proteins (Fig. 3 *c* and Fig. 4 *b*, respectively). As for LH1-RC from *Rb. veld.*, an extremely small amount of solubilized proteins, 1.5 pmol of LH1-RC and 0.9 pmol of LH2, was enough for successful incorporation at high protein density.

Finally, experiments using 0.3 mM DDM instead of DOTM to destabilize the SLB revealed that DDM also triggered direct incorporation of core complexes of *Rb. veld.* in SLB. In that case, high protein densities were obtained, although protein-containing domains were of smaller size than those with DOTM (data not shown).

Membrane remodeling on incubation

The samples reconstituted at room temperature were analyzed by AFM over several days. Between AFM experiments, samples were stored at 4°C. We observed 1 day after reconstitution, i.e., after an overnight incubation at 4°C and the equilibration time of the fluid cell at room temperature before AFM analysis, important changes in shape and composition of domains indicating a lateral diffusion of lipids and proteins in the reconstituted bilayer (Fig. 3 *b* compared to Fig. 2 *c*). This resulted in protein segregation into areas containing proteins in close contact surrounded by lipid domains. Topographs in oscillating mode revealed that more

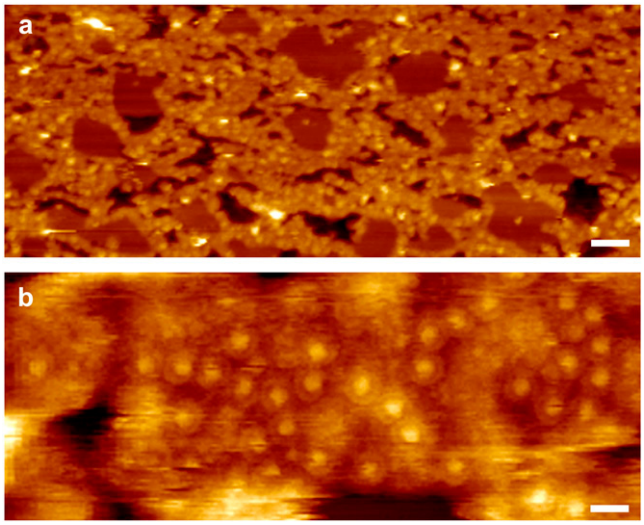

FIGURE 5 Direct incorporation of LH1-RC from *Rb. velk.* at 4°C. SLB was preincubated at 4°C with 0.025mM DOTM followed by incubation with 0.075 mM DOTM and 1.5 pmol of LH1-RC before detergent removal. (*a*) Low-magnification AFM contact mode of the reconstituted SLB with DPPC (*light brown*) and protein-containing domains (*yellow*). Only small domains (*dark*) of the initial SLB have been solubilized, as compared to similar reconstitution at room temperature. (*b*) High-resolution contact-mode AFM topograph of full LH1-RC complexes. The *z* color scale is 20 nm (*a*) or 10 nm (*c*), the darker areas corresponding to the mica. Scale bars are 100 nm in *a* and 10 mn in *b*.

than 85% of the core complexes contained the H subunits topping the RCs and protruding 3.2 ± 0.43 nm ($n = 11$) above the lipid bilayer (Fig. 3 *b*). This demonstrated that most of the proteins were incorporated with a unique orientation into the lipid bilayer.

We also observed important remodeling of SLB containing core complexes and LH2 from *pufX*$^-$ *Rb. sph.* on storage at 4°C. This led to flat areas close packed suitable for high-resolution AFM analysis in contact mode. As shown in the case of LH1-RC, the 16 α/β-heterodimers of the LH1 ring (9.2 ± 1.2 nm, $n = 21$) were resolved by image averaging (Fig. 3 *c*).

LH2-containing SLB show three membrane subdomains with different heights (Fig. 4 *a*). The flat and darker domains corresponded to the DOPC fluid phase alternating with flat DPPC domains protruding ~1 nm above the DOPC phase. Corrugated domains were constituted of LH2 that protruded ~1.5 nm above the DOPC phase. The nonameric subunits organization of LH2 (top ring diameter of 5.1 ± 0.27 nm, $n = 28$) was directly accessed in raw images (Fig. 4 *b*).

Direct incorporation of proteins into SLB at 4°C

Incorporation at 4°C of LH1-RC in 0.075 mM DOTM after 15 min incubation led to less incorporated proteins in SLB than at 20°C. This could be related to the slow equilibration of SLB with detergent at 4°C leading to a too low concentration of detergent within the SLB. We thus preincubated SLB at 4°C for 30 min with DOTM below the cmc at 0.025 mM, followed by incubation in the presence of protein in 0.075 mM DOTM. In this condition, high protein incorporation was observed (Fig. 5). Furthermore, SLB was less solubilized, presenting a continuous bilayer along micrometers with only few holes as compared to the reconstituted bilayer at 20°C, likely because of a lower solubilization effect of detergent at 4°C. Again, proteins were unidirectionally incorporated at high density as seen by topographs at low loading force in contact mode preserving the H subunits in all complexes (Fig. 5 *b*).

DISCUSSION

Previous studies of direct incorporation of proteins at low density into liposomes in solution have shown that the key parameter is the saturation of the liposome bilayer, i.e., just before the onset of solubilization, by sugar-based detergents, OG or DDM (reviewed by Rigaud et al. (16)). The application of these data to a planar lipid bilayer led us to incubate SLB with the maximal amount of detergent, DDM or DOTM, before the full solubilization, and, under these conditions, high protein incorporation was obtained. No protein incorporation as seen by AFM was obtained after destabilization of SLB with a lower amount of detergent, e.g., 0.01–0.02 mM DOTM. However we cannot exclude that proteins were inserted but at low density, as already reported by spectroscopic analysis (26) or by single-molecule fluorescence imaging (15) of membrane protein incorporated using detergent well below the cmc.

Reconstituted bilayers are flat and interconnected along microns without bound vesicles on the lipid bilayer or on the mica (Fig. 2 *a*), ruling out a mechanism of reconstitution in bulk from solubilized protein and lipid followed by a fusion step of proteoliposomes onto the mica. Proteins are incorporated into the DOPC domains (Figs. 2 *b* and 4 *a*), likely because of the fluid packing, and are able to diffuse with time incubation, leading to segregation of proteins into protein close-packing areas (Fig. 3). Here, both DPPC gel and DOPC fluid phases have been used to facilitate the AFM analysis by highlighting SLB, but we suggest performing future experiments with a pure fluid lipid phase.

Heights measurements of LH2 and raw images of LH1-RC of the extramembraneous domains protruding from the bilayer show that proteins were unidirectionally incorporated in the lipid bilayer. The cytoplasmic H subunit of ~3 nm height topping the RC in the LH1-RC complex observed in the raw data reveal that the proteins were incorporated in the lipid bilayer through the periplasmic domain (1.2 nm height (25)). The LH2 complexes protrude ~1.5 nm out of the bilayer, a value consistent with the height of the periplasmic domain of ~1 nm, the cytoplasmic domain pointing out ~0.3 nm, as reported from AFM analysis of 2D crystals (24). Hence, although both complexes contain cytoplasmic and

periplasmic domains pointing out of the bilayer, incorporation occurs within the hydrophobic lipidic environment through the less bulky or less charged extramembranous domain. The same conclusion was drawn from studies of direct incorporation into liposomes of highly hydrophobic membrane proteins such as bacteriorhodopsin or those containing a large extramembranous domain protein such as FOF1 ATPase (12, 16).

The protein-containing bilayers are small, ~200 nm × 200 nm, compared to classical 2D crystals and might be improved by a better handling of the experimental conditions. However, they are connected along microns to each other, drastically decreasing the lateral mobility on scanning compared to adsorbed vesicles of similar size, allowing high-resolution topographs to be recorded. Thus, this approach appears to present an alternative to the AFM analysis of 2D crystals obtained by detergent removal from fully solubilized lipids and proteins. Here, large integral protein complexes of different size LH2 (110 kDa) and LH1-RC (290 kDa) have been incorporated, and we believe that proteins up to similar sizes could be incorporated. Several methods of formation of planar lipid bilayers containing proteins involve a tethered bilayer, leaving a thickness of several nanometers between the bilayer and the mica, to favor protein incorporation. Here, we show that LH1-RC complexes with their periplasmic side of 1.2 nm height facing the mica are incorporated and can diffuse within the lipid bilayer (Fig. 3). We thus consider that at least a water layer of a similar height is present between the mica and the lipid bilayer. SLB thickness measured in our conditions was higher than 6.15 nm, suggesting a 1.7 nm water layer between mica and lipid polar heads considering a 4.42 nm thickness for a DPPC bilayer (21). The presence of such a water layer with a thickness ranging up to 3 nm has been well established (27). Finally, analysis of the atomic structures of membrane proteins from the different families, e.g., the large families of porins, ABC transporters, or secondary transporters reported in the Membrane Protein Data Bank (http://blanco.biomol.uci.edu/Membrane_Proteins_xtal.html) revealed that the vast majority of proteins are highly asymmetric with the smallest extramembranous domains of ~1–2 nm.

A major interest of this method is the extremely small amount of protein needed to obtain a high protein density in the lipid bilayer. Incorporations have been obtained starting with ~1 pmol (0.1 μg for LH2) of solubilized protein, and a total of 30 picomoles of proteins has been needed for all the experiments reported here. This is the consequence of the incorporation of proteins present in the bulk into the planar surface. An accurate measurement of the total amount of incorporated protein is complicated by the large size of the SLB. However, we propose that the picomole range of protein is close to the minimum amount required to ensure a high protein density in the SLB. Indeed, for a membrane protein such as LH1-RC with a ~10 nm diameter and a SLB covering the 10-mm mica, we can estimate that 1 pmol of protein is needed to saturate the SLB. Moreover, only ~50% of the previous lipid bilayer is available because proteins are not incorporated in the DPPC domains and SLB is partly solubilized by the detergent. However, this approach clearly requires the lowest amount of material, as compared to alternative methods in membrane structural biology. For comparison, 2D crystallizations in bulk or at the air-water interface require 25–50 μg protein and 1–2 μg protein per trial (28,29), respectively, and the conditions of crystallization should be found varying several parameters. Other methods of reconstitution into planar bilayer have reported micromolar protein concentrations (30,31).

CONCLUSION

Here, we have reported a new method for directly incorporating purified membrane proteins into detergent-destabilized planar lipid bilayers. Proteins are unidirectionally incorporated at protein close-packing densities within the SLB, allowing high-resolution AFM of three photosynthetic membrane proteins to be recorded.

This method is experimentally simple and versatile, involving only commercially available compounds, namely lipids and detergents. The mechanism of incorporation that drives the solubilized proteins into the more favorable lipidic environment is a fast process, taking a few minutes at room temperature or at 4°C. The concentration of solubilized protein is extremely low, and thus, proteins could be incorporated just after the purification step without any concentration step. Here, stable membrane proteins were incorporated, but it is thus likely that purified proteins less stable in detergent could be functionally incorporated. Indeed, reconstitution into liposomes for functional studies and 2D crystallization for structural analysis usually involved a detergent removal of several hours by days by dialysis. Hence, although our report focused on the structural analysis of proteins by AFM, we believe that these technical characteristics combined with the unique orientation of protein into the bilayer would allow further applications in the biomaterials field involving membrane proteins.

This study was supported by the European Community (IHP-RTN), the Human Frontier Science Program (to F.G.), the Commissariat Français à l'Energie Atomique (Nuclear Toxicology Program, to A.B.), and the Centre National de la Recherche Scientifique (ACI DRAB Cibles Thérapeutiques, Ministère de la Recherche, to P.E.M.).

REFERENCES

1. Tate, C. G., J. Haase, C. Baker, M. Boorsma, F. Magnani, Y. Vallis, and D. C. Williams. 2003. Comparison of seven different heterologous protein expression systems for the production of the serotonin transporter. *Biochim. Biophys. Acta.* 1610:141–153.
2. Auer, M., G. A. Scarborough, and W. Kuhlbrandt. 1998. Three-dimensional map of the plasma membrane H^+-ATPase in the open conformation. *Nature.* 392:840–843.

3. Levy, D., G. Mosser, O. Lambert, G. Moeck, D. Bald, and J. L. Rigaud. 1999. Two-dimensional crystallization on lipid layer: A successful approach for membrane proteins. *J. Struct. Biol.* 127:44–52.

4. Engel, A., H. E. Gaub, and D. J. Muller. 1999. Atomic force microscopy: a forceful way with single molecules. *Curr. Biol.* 9: R133–R136.

5. Stahlberg, H., A. Engel, and A. Philippsen. 2002. Assessing the structure of membrane proteins: combining different methods gives the full picture. *Biochem. Cell Biol.* 80:563–568.

6. Muller, D. J., G. M. Hand, A. Engel, and G. E. Sosinsky. 2002. Conformational changes in surface structures of isolated connexin 26 gap junctions. *EMBO J.* 21:3598–3607.

7. Scheuring, S., J. Seguin, S. Marco, D. Levy, B. Robert, and J. L. Rigaud. 2003. Nanodissection and high-resolution imaging of the *Rhodopseudomonas viridis* photosynthetic core complex in native membranes by AFM. Atomic force microscopy. *Proc. Natl. Acad. Sci. USA.* 100:1690–1693.

8. Oesterhelt, F., D. Oesterhelt, M. Pfeiffer, A. Engel, H. E. Gaub, and D. J. Muller. 2000. Unfolding pathways of individual bacteriorhodopsins. *Science.* 288:143–146.

9. Janovjak, H., M. Kessler, D. Oesterhelt, H. Gaub, and D. J. Muller. 2003. Unfolding pathways of native bacteriorhodopsin depend on temperature. *EMBO J.* 22:5220–5229.

10. Fotiadis, D., Y. Liang, S. Filipek, D. A. Saperstein, A. Engel, and K. Palczewski. 2003. Atomic-force microscopy: Rhodopsin dimers in native disc membranes. *Nature.* 421:127–128.

11. Scheuring, S., D. Levy, and J. L. Rigaud. 2005. Watching the components of photosynthetic bacterial membranes and their in situ organisation by atomic force microscopy. *Biochim. Biophys. Acta.* 1712:109–127.

12. Rigaud, J. L., and D. Levy. 2003. Reconstitution of membrane proteins into liposomes. *Methods. Enzymol.* 372:65–86.

13. Sinner, E. K., U. Reuning, F. N. Kok, B. Sacca, L. Moroder, W. Knoll, and D. Oesterhelt. 2004. Incorporation of integrins into artificial planar lipid membranes: characterization by plasmon-enhanced fluorescence spectroscopy. *Anal. Biochem.* 333:216–224.

14. Tanaka, M., and E. Sackmann. 2005. Polymer-supported membranes as models of cell surface. *Nature.* 437:656–663.

15. Smith, E. A., J. W. Coym, S. M. Cowell, T. Tokimoto, V. J. Hruby, H. I. Yamamura, and M. J. Wirth. 2005. Lipid bilayers on polyacrylamide brushes for inclusion of membrane proteins. *Langmuir.* 21:9644–9650.

16. Rigaud, J., B. Pitard, and D. Levy. 1995. Reconstitution of membrane proteins into liposomes: application to energy-transducing membrane. *Biochim. Biophys. Acta.* 1231:223–246.

17. Francia, F., J. Wang, G. Venturoli, B. A. Melandri, W. P. Barz, and D. Oesterhelt. 1999. The reaction center-LH1 antenna complex of *Rhodobacter sphaeroides* contains one PufX molecule which is involved in dimerization of this complex. *Biochemistry.* 38:6834–6845.

18. Milhiet, P., M. C. Giocondi, O. Baghdadi, F. Ronzon, B. Roux, and C. Le Grimellec. 2002. Spontaneous insertion and partitioning of alkaline phosphatase into model lipid rafts. *EMBO Rep.* 3:485–490.

19. Marabini, R., I. M. Masegosa, M. C. San Martin, S. Marco, J. J. Fernandez, L. G. de la Fraga, C. Vaquerizo, and J. M. Carazo. 1996. Xmipp: an image processing package for electron microscopy. *J. Struct. Biol.* 116:237–240.

20. Giocondi, M. C., V. Vie, E. Lesniewska, P. E. Milhiet, M. Zinke-Allmang, and C. Le Grimellec. 2001. Phase topology and growth of single domains in lipid bilayers. *Langmuir.* 17:1653–1659.

21. Seelig, J., and A. Seelig. 1980. Lipid conformation in model membranes and biological membranes. *Q. Rev. Biophys.* 13:19–61.

22. Nagle, J. F., and S. Tristam-Nagle. 2000. Structure of lipid bilayers. *Biochim. Biophys. Acta.* 1469:159–195.

23. Walz, T., and R. Ghosh. 1997. Two-dimensional crystallization of the light-harvesting I-reaction centre photounit from *Rhodospirillum rubrum*. *J. Mol. Biol.* 265:107–111.

24. Scheuring, S., J. Seguin, S. Marco, D. Levy, C. Breyton, B. Robert, and J. L. Rigaud. 2003. AFM characterization of tilt and intrinsic flexibility of *Rhodobacter sphaeroides* light harvesting complex 2 (LH2). *J. Mol. Biol.* 325:569–580.

25. Fotiadis, D., P. Qian, A. Philippsen, P. A. Bullough, A. Engel, and C. N. Hunter. 2004. Structural analysis of the reaction center light-harvesting complex I photosynthetic core complex of *Rhodospirillum rubrum* using atomic force microscopy. *J. Biol. Chem.* 279:2063–2068.

26. Tollin, G., Z. Salamon, S. Cowell, and V. Hruby. 2003. Plasmon-waveguide resonance spectroscopy: a new tool for investigating signal transduction by G-protein coupled receptors. *Life Sci.* 73:3307–3311.

27. Sackmann, E. 1996. Supported membranes: scientific and practical applications. *Science.* 271:43–48.

28. Auer, M., G. A. Scarborough, and W. Kuhlbrandt. 1999. Surface crystallisation of the plasma membrane H^+-ATPase on a carbon support film for electron crystallography. *J. Mol. Biol.* 287:961–968.

29. Levy, D., M. Chami, and J. L. Rigaud. 2001. Two-dimensional crystallization of membrane proteins: the lipid layer strategy. *FEBS Lett.* 504:187–193.

30. Ataka, K., F. Giess, W. Knoll, R. Naumann, S. Haber-Pohlmeier, B. Richter, and J. Heberle. 2004. Oriented attachment and membrane reconstitution of His-tagged cytochrome *c* oxidase to a gold electrode: in situ monitoring by surface-enhanced infrared absorption spectroscopy. *J. Am. Chem. Soc.* 126:16199–16206.

31. Rigler, P., W.-P. Ulrich, and H. Vogel. 2004. Controlled immobilization of membrane proteins to surfaces for FTIR investigations. *Langmuir.* 20:7901–7903.